NMR Analysis of Interactions of a Phosphatidylinositol 3′-Kinase SH2 Domain with Phosphotyrosine Peptides Reveals Interdependence of Major Binding Sites†

Ulrich L. Günther, Yuxi Liu, David Sanford, William W. Bachovchin, and Brian Schaffhausen*

Department of Biochemistry, Tufts University School of Medicine, 136 Harrison Avenue, Boston, Massachusetts 02111

Received July 19, 1996; Revised Manuscript Received October 2, 1996⊗

ABSTRACT: The interactions of the N-terminal src homology (SH2) domain (N-SH2) of the 85 kDa subunit of phosphatidylinositol 3′-kinase (PI-3K) with phosphotyrosine (ptyr) and a series of ptyr-containing peptides have been examined by NMR spectroscopy. HSQC (heteronuclear single-quantum coherence) NMR spectra of ^{15}N-labeled SH2 were used to evaluate its interactions with ptyr-containing ligands. The ability of ligands to cause chemical shift changes was compared to their potency as competitors in *in vitro* binding experiments using polyoma virus middle T antigen (MT). The results suggest the interdependence of SH2 binding elements. Chemical shifts of residues involved in the ptyr binding were altered by variations of the sequence of the bound peptide, suggesting that the ptyr fit can be adjusted by the peptide sequence. Perturbations of chemical shifts of residues coordinating the methionine three residues C-terminal to the ptyr (the +3 residue) were affected by substitution in the binding peptide at +1 and vice versa. Such results show synergistic interplay between regions of the SH2 binding residues C-terminal to the ptyr.

Src homology 2 (SH2)[1] domains are protein modules through which tyrosine phosphorylation regulates cellular processes (Cohen et al., 1995; Marengere & Pawson, 1994; Schaffhausen, 1995; Schlessinger, 1994). SH2s respond to tyrosine phosphorylation by binding the tyrosine-phosphorylated sequences. These elements, containing approximately 100 amino acids, have now been found in more than 100 proteins. Biochemical, genetic, and structural approaches have been used to examine the basis for their specificity. Consensus sequences have been observed in proteins that bind particular SH2s (Cantley et al., 1991). *In vitro* peptide selections by isolated SH2s have been used to compare preferred binding sequences (Songyang et al., 1993, 1994). Such studies demonstrate that residues C-terminal to the ptyr are important for binding. Both X-ray diffraction and NMR have been used to establish the structure of particular SH2−tyrosine phosphopeptide complexes (Eck et al., 1993; Hatada et al., 1995; Lee et al., 1994; Overduin et al., 1992; Pascal et al., 1994; Waksman et al., 1993; Xu et al., 1995; Zhou et al., 1995; Nolte et al., 1996). The structure of the SH2 can be described as a central antiparallel β-sheet flanked by smaller β-sheets and two α-helices (Figure 1A). The peptide binding function of the SH2 has been described as a prong and socket (Waksman et al., 1993).

This work focuses on PI 3′-kinase, a key enzyme in signal transduction pathways. PI 3′-kinase associates with almost all activated tyrosine kinases (Cantley et al., 1991). Its importance has been demonstrated in systems of both normal and oncogenic growth regulation. PI 3′-kinase is, for example, a downstream mediator of the mitogenic signal of the PDGF receptor (PDGFr) (Fantl et al., 1992; Valius et al., 1993). Our interest arose through its interactions with polyoma virus middle T antigen. Polyoma virus transforms cells *in vitro* and induces a broad range of tumors in mice. Both *in vitro* transformation (Carmichael et al., 1984) and *in vivo* tumor induction (Freund et al., 1992) are drastically affected when middle T is mutated to abolish PI 3′-kinase binding.

Most forms of PI 3′-kinase are heterodimers consisting of a catalytic 110 kDa subunit and an 85 kDa regulatory subunit (Carpenter et al., 1990). The association of the p85 subunit with middle T was shown to depend upon tyrosine phosphorylation of middle T at residue 315 and to result in translocation of the enzyme from cytosolic to membrane fractions (Cohen et al., 1990a,b). Cloning of the p85 subunit showed the presence of two SH2 domains. Either of the two SH2 domains of the p85 subunit will bind the sequence around the tyrosine phosphorylation site at residue 315 of middle T (Yoakim et al., 1992). A similar situation is observed with the PDGFr where sequences around tyrosine phosphates at 740 and 751 mediate interactions with p85 SH2s (Escobedo et al., 1991; Kashishian et al., 1992).

The N-terminal SH2 (N-SH2) of p85 has been used as a model for genetic, biochemical, and structural studies of SH2 function. Peptide selection experiments indicated that the p85 N-SH2 (p85N) has a preference for binding pY[MVIE]-XM sequences (Songyang et al., 1993). This is consistent with the pYMPM sequence found in middle T or the pYVPM/pYMDM sequences of the PDGF receptor. In SH2 domain structures such as src and p85, αA2 (p85N: R340) and βB5 (p85N: R358) are involved in coordinating the

† This work was supported by NIH Grants CA34722 and CA50661 as well as by the Markey Foundation.

* Author to whom correspondence should be addressed: telephone, 617-636-6876; FAX, 617-636-6409; e-mail, bschaffh_pol@opal.tufts.edu.

⊗ Abstract published in *Advance ACS Abstracts,* November 15, 1996.

[1] Abbreviations: Src, sarcoma family of nonreceptor kinases; SH2, src homology 2; PDGF and PDGFr, platelet-derived growth factor and PDGF receptor; PI-3K, phosphatidylinositol 3′-kinase; MT, middle tumor antigen; GST, glutathione *S*-transferase; pY, ptyr, phosphotyrosine; Ac-pY-NH_2, acetylphosphotyrosine amide; SDS, sodium dodecyl sulfate; 2D and 3D, two and three dimensional; INEPT, insensitive nuclei enhanced by polarization transfer; HMQC, heteronuclear multiquantum coherence; HSQC, heteronuclear single-quantum coherence; NOESY, nuclear Overhauser effect spectroscopy; TOCSY, total correlation spectroscopy; TPPI, time-proportional phase incrementation.

S0006-2960(96)01783-7 CCC: $12.00

phosphate of the ptyr. Mutation of R358 has confirmed its importance (Yoakim et al., 1994).

The methionine at +3 C-terminal to the ptyr is coordinated by a hydrophobic pocket including the EF loop. Consistent with this, the mutation of EF3 residue P395 to S led to reduced binding of middle T and an inability to select peptides containing methionine at +3 from degenerate libraries (Yoakim et al., 1994).

The goal of this study was to map the interactions of a series of phosphorylated peptides with the N-SH2 of p85. For this purpose, the backbone of the SH2 was assigned using ^{15}N-labeled SH2. Changes of chemical shifts in HSQC spectra caused by peptide binding were correlated to alterations in the sequence of the bound peptide. ^{1}H and ^{15}N chemical shift changes observed in HSQC spectra are caused by interactions or rearrangements that alter the magnetic environment of backbone atoms. Such chemical shift changes have frequently been used to map ligand interactions to particular sites on proteins (Chen et al., 1992; Spitzfaden et al., 1992; Coombs et al., 1996; Otting, 1993). Our results support the previously established importance of the ptyr binding pocket and the hydrophobic binding site for the +3 position of the peptide. They also indicate strong mutual interdependence of the binding elements of the SH2.

MATERIALS AND METHODS

Clones and Viruses. A pGEX 3X−glutathione *S*-transferase−N-SH2 construct (amino acids 321−434) was used to produce SH2 for NMR analysis (Yoakim et al., 1992). Middle T antigen (MT) and pp60^{c-src} expressing baculoviruses were propagated on Sf9 cells in Grace's medium (10% fetal bovine serum) (Cohen et al., 1990a,b). Typically, infected cells were used 40 h postinfection. Middle T was immunoprecipitated using rabbit peptide antiserum against middle T residues 280−302.

Preparation of p85 N-SH2. ^{15}N-Labeled SH2 has been prepared using either rich medium (Celtone U, Martek) or minimal medium prepared with $^{15}NH_4Cl$ (Cambridge Isotope Laboratories). The resulting proteins gave identical NMR spectra, although minimal medium yielded slightly better ^{15}N incorporation (>90%). For growth on minimal medium, a 500 mL culture of *Escherichia coli* (JM109) was grown overnight in Luria−Bertani broth. Cells were pelleted and grown in 2000 mL of minimal medium containing 1 g/L $^{15}NH_4Cl$ until the OD at 600 nm was equal to or above 1.0. Isopropyl β-D-thiogalactoside was added to 100 μM and incubation carried out 6−8 h at 30 °C. Cells were collected at 4000*g* for 5 min. The Celtone U medium was reused for a second cycle of growth to maximize protein yield with the enriched medium. Pooled cell pellets were divided into eight tubes, and 20 mL of PBS$^-$ was added to each. Sonication was then performed in a Branson sonifier for 1 min intervals until most cells were disrupted. A 10% volume of 10% Triton X-100 was then added. After centrifugation at 10000*g*, pooled supernatants were then incubated with glutathione agarose beads (Sigma) for 30 min at room temperature. The beads were washed three times with phosphate-buffered saline (PBS). The cell pellet and supernatant were checked by gel electrophoresis and reextracted or treated with more glutathione beads if necessary. Approximately 120 mg of fusion protein was obtained.

Factor Xa was used to cleave the SH2 from the fusion protein. The glutathione beads were washed first with 50 mM Tris-HCl, pH 7.5/150 mM NaCl and then with the same buffer with 1 mM $CaCl_2$. Factor Xa (500 μg) (Hematologic Technologies) was then used to cleave the SH2 overnight at room temperature. The supernatant contained the SH2 fusion. The SH2 was further purified by chromatography on Sephadex G50. A 3−5 mL sample containing 20−25 mg of protein was loaded on a 1000 mm × 25 mm column. Elution at 1.5 mL/min was carried out with 0.1 mM KCl, pH 6.8/0.02% sodium azide. Fractions (4−5 mL) were monitored at 280 nm. Purified SH2 was soluble at concentrations of several millimolar and stable for long periods (at least 10 weeks) at 35 °C and pH 6.5−7.0. No buffer was added to the NMR sample to avoid unpredictable interactions. The pH was adjusted by careful titration with 0.25 M HCl/NaOH.

Phosphotyrosine and Phosphotyrosine-Containing Peptides. Phosphotyrosine (pY) was obtained from Sigma; acetylphosphotyrosine amide (Ac-pY-NH_2) was the kind gift of Sheldon Ratnofsky of BASF Bioresearch Corp. pYM-NH_2 and different peptides were synthesized by the Tufts Protein Chemistry Facility. Peptides were purified on a Waters LC4000 HPLC using a Vydac C18 column with water/acetonitrile/0.1% TFA solvent. Peptides were used from the middle T sequence around the tyrosine phosphorylation site at residue 315, EEEY$_{315}$MPME-NH_2, EEEpY$_{315}$MPME-NH_2, EEEpY$_{315}$MPMEDLYLDIL-NH_2, EEEpY$_{315}$GPME-NH_2, EEEpY$_{315}$MGME-NH_2, EEEpY$_{315}$MPGE-NH_2, EEEY$_{315}$APME-NH_2, and EEEpY$_{315}$MPAE-NH_2, or SVD-pYVPML-NH_2 from the 751 phosphorylation site of the PDGF receptor.

Binding Assays with Middle T. Middle T used in the binding experiments was labeled with [^{32}P]PO_4 as described previously (Yoakim et al., 1994). Sf9 cells coinfected with middle T and src baculoviruses were extracted with an NP40-containing buffer [0.137 M NaCl, 0.01 M Tris-HCl (pH 9.0), 0.001 M $MgCl_2$, 0.001 M $CaCl_2$, 10% (v/v) glycerol, 1% (v/v) Nonidet P-40]. The extracts were incubated with protein A−Sepharose beads and MT polyclonal antibody for 1 h on ice. Washed immunoprecipitates were incubated for 15 min at room temperature in 20 mM Tris-HCl (pH 7.5)/5 mM $MnCl_2$ with [γ-^{32}P]ATP (2000 Ci/mmol, NEN). After the reactions were washed with PBS, 0.5 M LiCl, and water, beads were boiled for 2 min in a solubilization buffer containing 0.4% sodium dodecyl sulfate, 50 mM triethanolamine (pH 7.4), 100 mM NaCl, and 2 mM 2-mercaptoethanol. After boiling, the samples were spun out, the supernatant was collected, and iodoacetamide was added to a final concentration of 10 mM. Finally, one-fourth volume of 10% Triton X-100 was added, and MT was reimmunoprecipitated from these supernatants with protein A−Sepharose and MT antibody for 1 h on ice. The reactions were washed again and the dry beads frozen. MT was boiled in solubilization buffer as described above as needed.

For competition experiments, p85 N-SH2 fusion proteins on glutathione beads were incubated with different competitors for 10 min at 4 °C. ^{32}P-Labeled middle T was then added, and the reaction was allowed to continue for 1 h on ice. After incubation, the beads were washed once with PBS, twice with 0.5 M LiCl, and one last time with PBS. The buffers of the last two washes contained 100 μg/mL bovine serum albumin which prevented the beads from sticking to the tubes. The samples were then boiled in SDS sample buffer and run on 7.5% SDS−PAGE. The gels were stained with Coomassie Brilliant Blue and then dried. The middle

T bound was analyzed using a Molecular Dynamics Phosphorimager.

NMR Analysis. NMR data were acquired on a Bruker AMX500 NMR spectrometer employing a 5 mm triple resonance inverse probe. The water signal was suppressed using either a 1.8 ms Messerle pulse (Messerle et al., 1989) for all 2D and 3D HSQC experiments or a soft-pulse presaturation during recycle delays (Campbell et al., 1974) for 3D NOESY- and TOCSY-HMQC experiments [$1/(2J_{NH}) = 4.6$ ms]. Pure absorption mode phase-sensitive spectra were obtained using the mixed mode States−TPPI method (Marion & Wüthrich, 1983). The proton sweep width was 7575 Hz. A nitrogen sweep width of 1700 Hz was chosen to avoid chemical shift degeneracy caused by the folding of the arginine side chain H^{ϵ} peaks. Frequency offsets O1(^{1}H) and O2(^{15}N) were 9130 and 4515 Hz, respectively. Additional spectra with a nitrogen sweep width of 5000 Hz allowed the detection of unfolded Arg H^{ϵ} signals. Assignments were obtained primarily from 3D ^{1}H−^{15}N NOESY-HMQC or HSQC and ^{1}H−^{15}N TOCSY-HMQC (Marion et al., 1989) spectra of 2 mM free and EEEpYMPME-NH_2 complexed SH2.

Initially HSQC spectra of the free SH2 and the EEEpYMPME-NH_2 complex were recorded at 308.8, 303.8, 298.8, and 293.8 K. The data reported here were from spectra recorded at 308.8 K. Spectra recorded at different temperatures showed no substantial differences. The pH of the NMR samples was adjusted to 6.8 (±0.1) by addition of 0.25 M sodium hydroxide or hydrochloric acid to the protein and to the peptide solution and was monitored before and after recording each spectrum. No pH changes were observed for free and inhibited SH2s over long periods of time.

HSQC or double-refocused INEPT spectra (Bax et al., 1990) were used to probe protein−peptide interactions. Concentrations of the SH2s used for peptide titrations were as low as 0.3 mM. Peptide titrations were monitored by ^{1}H-^{15}N HSQC spectra of the SH2 complex until saturation was reached.

FELIX2.3 (Biosym Technologies) was used for data processing. Typical window functions were a Gaussian−Lorentzian multiplication (Lorentzian broadening = −8, Gaussian broadening ranging from 0.05 to 0.1) for the recorded dimension and a cubic sinebell shifted by 70° for the incremented dimension. Linear prediction was employed for the ^{15}N dimension in 3D and in some 2D HSQC spectra. Proton chemical shifts were referenced to the aqueous solvent peak at 4.772 ppm at 25 °C employing a temperature coefficient of 0.0115/1 °C as described by Wishart et al. (1995). ^{15}N chemical shifts were determined relative to the ^{1}H reference based on previous referencing to NH_3. Temperature dependency of ^{15}N chemical shifts was neglected.

RESULTS

Peptide Affinities. The p85 N-SH2 (residues 321−434) was expressed as a GST fusion protein using a pGEX-3X construct. Figure 1B shows the sequence of the SH2 using the nomenclature suggested by Eck et al. (1993). As expected (Yoakim et al., 1992), this SH2 fusion bound [^{32}P]-tyrosine-phosphorylated middle T in an *in vitro* binding assay (Figure 2). The binding of ^{32}P middle T was blocked by addition of a tyrosine-phosphorylated peptide (EEEpYMPME-NH_2) matching the sequence of the middle T tyrosine

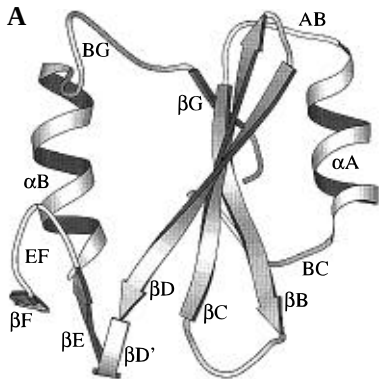

B

```
321       330       340       350       360
|         |         |         |         |
GMNNNMSLQDAEWYWGDISREEVNEKLRDTADGTFLVRDA
          βA AA     αA        AB    βB

          370       380       390
          |         |         |
STKMHGDYTLTLRKGGNNKSIKIFHRDGKYGFSDPLTFN
  BC    βC    CD    βD    βD'DE βE EF βF

400       410       420       430
|         |         |         |
SVVELINHYRNESLAQYNPKLDVKLLYPVSKYQQD
    αB          BG        βG
```

FIGURE 1: (A) Richardson diagram of p85 N-SH2, revised from data of Booker et al. (1992). SH2s have a central antiparallel β-sheet flanked by two α-helices. Peptides bind orthogonal to the central sheet with the phosphotyrosine to the right. The designation of structural elements follows the description of Eck et al. (1993). (B) Sequence of the p85 N-SH2 construct. The SH2 sequence is shown in boldface.

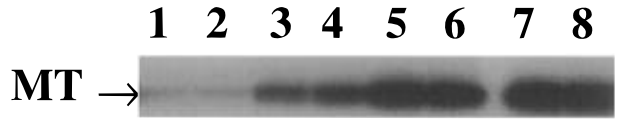

FIGURE 2: MT binding and example of competition. [^{32}P]Tyrosine-phosphorylated middle T was incubated with GST−p85 N-SH2 in the presence of decreasing concentrations of EEEpYMPME-NH_2 (1−6) or alone (7−8) as described in Materials and Methods. After washing and SDS−PAGE, bound middle T was visualized by the Molecular Dynamics Phosphorimager. Lanes: 1 and 2, 12.5 μM EEEpYMPME-NH_2; 3 and 4, 4.2 μM EEEpYMPME-NH_2; 5 and 6, 1.4 μM EEEpYMPME-NH_2; 7 and 8, no peptide addition.

phosphorylation site at residue 315. In competition assay, this peptide reduced middle T binding to the N-SH2 with an IC_{50} of 8.4 μM. Since the N-SH2 of p85 is known to bind middle T at residue 315 (Cohen et al., 1990a,b; Yoakim et al., 1992), this observation was expected. Ac-pY-NH_2, pYM-NH_2 and a series of peptide variants derived from middle T around the phosphorylation site at 315 (EEEpYMPME-NH_2) were compared for their ability to block middle T binding in the same competition assay. Table 1 shows the IC_{50}s determined. A simple phosphotyrosine derivative (Ac-pY-NH_2) gave an IC_{50} of 4.3 mM. IC_{50} values for the peptides ranged between 4.8 mM for the unphosphorylated MT peptide and 6.1 μM for EEEpYMPMED-LYLDIL-NH_2. In the peptide series, the absence of phosphate on Y315 increased the IC_{50} to above 1.5 mM. Residues N-terminal to the ptyr or C-terminal to the +4 residue were not critical, contributing only a little to overall affinity. As expected from usual models of SH2 behavior, the +2 position also contributed little. However, substitution of +1 or +3 with glycine increased the IC_{50} above millimolar. Substitution of alanine at +1 and +3 also reduced

Table 1: Comparison of Abilities To Block Middle T Binding to p85 N-SH2

compound	IC_{50} (μM)
acetylphosphotyrosine amide	4300
pY	21000
Ac-pYM-NH_2	7600
EEEY_{315}MPME-NH_2	4800
EEEpY_{315}MPME-NH_2	8.4
EEEpY_{315}MPMEDLYLDIL-NH_2	6.1
EEEpY_{315}**G**PME-NH_2	1250
EEEpY_{315}M**G**ME-NH_2	8.1
EEEpY_{315}MP**G**E-NH_2	>1250
EEEpY_{315}**A**PME-NH_2	33
EEEpY_{315}MP**A**E-NH_2	200
SVDpYVPML-NH_2 (PDGFr)	13.4

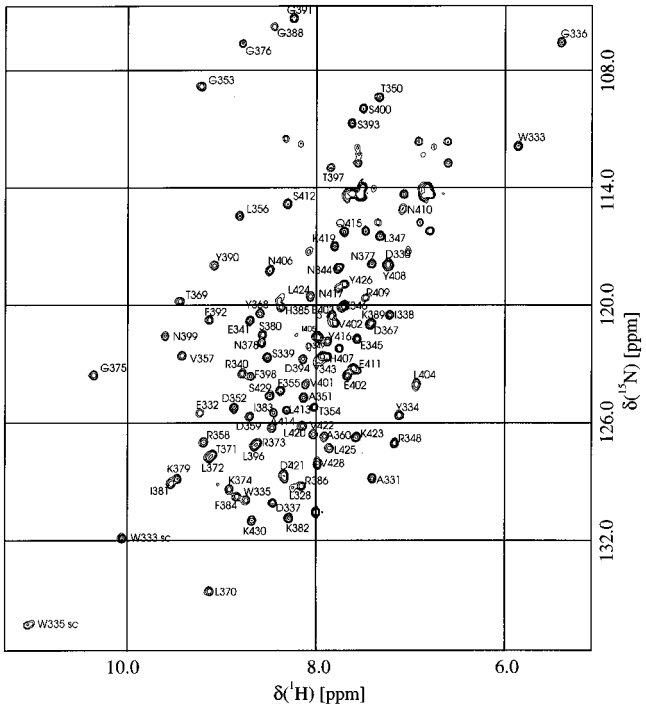

FIGURE 3: HSQC spectrum of p85 N-SH2.

affinity, but the effect was less drastic than for the glycine substitution. The competition experiments indicated that pY, the +1 or +3 but not the +2 position, makes substantial contributions to the affinities. This is consistent with peptide selection experiments (Songyang et al., 1993; Yoakim et al., 1994). For comparison, the PDGFr sequence around the tyrosine phosphorylation site at 751 was also tested and found to have a high affinity (IC_{50} of 13.4 μM).

Assignment of the $^1H-^{15}N$ HSQC Spectrum of p85 N-SH2. The GST−N-SH2 fusion protein was next prepared using ^{15}N-containing medium. After cleavage of the fusion with factor Xa, the SH2 domain was purified by chromatography. An $^1H-^{15}N$ HSQC spectrum exhibited more than 130 cross peaks representing peptide amides and some side chain resonances (Figure 3). The structure of a free bovine p85 N-SH2 was previously determined by Campbell and coworkers (Booker et al., 1992), who have also reported the assignments of the free and peptide-bound p85 N-SH2 (Hensmann et al., 1994). Because some of our chemical shifts are different from the frequencies reported by Hensmann et al., the entire spectrum was assigned *de novo,* primarily from ^{15}N-edited NOESY and TOCSY. Table 1 of the Supporting Information lists the backbone assignments. Differences between our and their data may be attributed to a number of factors: Their p85 SH2 had L in position 380

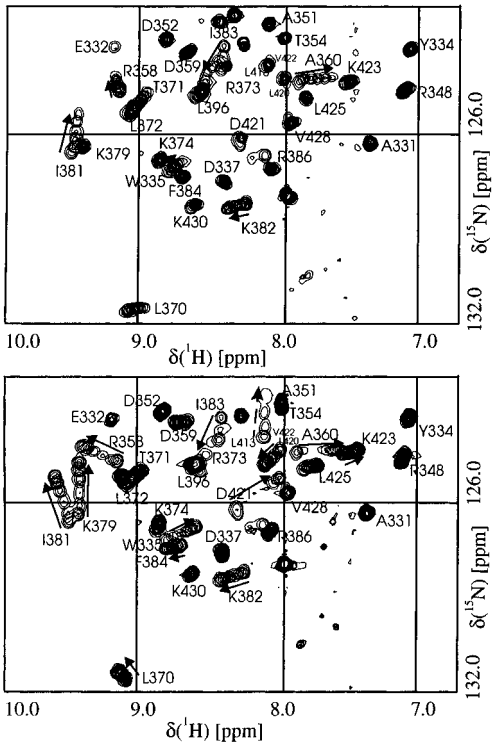

FIGURE 4: HSQC titrations. (Top) A section of superimposed $^1H-^{15}N$ HSQC spectra of p85 N-SH2 titrated with Ac-pY-NH_2. Six different steps are shown. Arrows indicate examples of chemical shift movement during the titration. (Bottom) Six steps in the titration of p85 N-SH2 with EEEpYMPME-NH_2.

where our SH2 had S (bovine vs rat SH2); their data were recorded at pH 5.8 whereas we chose pH 6.8; they used 50−80 mM phosphate buffer, which affected several signals of residues involved in peptide binding (S339, R340, E345, A360, G366, D367, Y368, I383, and R386).

N-SH2 Interactions with N-Acetylphosphotyrosine Amide. The major aim of this work was to compare binding of phosphotyrosine and a collection of phosphotyrosine-containing peptides to the p85 N-SH2. Ac-pY-NH_2 was used to probe for residues of p85 N-SH2 which are involved in the ptyr interaction. Figure 4 (top) shows a section out of six superimposed $^1H-^{15}N$ HSQC spectra representing successive stages of the ptyr titration. Titration was considered complete when addition of Ac-pY-NH_2 had no effect on the spectra. By carrying out such titrations, it was usually a simple matter to follow changes in positions of individual cross peaks. Table 2 of the Supporting Information lists ^{15}N and ^1H chemical shift changes observed for all complexes.

Figure 5 depicts chemical shift changes in HSQC spectra as a function of position in the SH2 sequence. Panels a and c report ^1H and ^{15}N chemical shift differences, respectively. Deciding what represents significant chemical shift changes is clearly a matter of judgment. For example, a study of the bacterial phosphotransferase system by Wright's laboratory (Chen et al., 1993) listed residues changing by $\delta(^1H)$ >0.04 ppm or $\delta(^{15}N)$ >0.2 ppm as significant; analysis of cyclosporin A/cyclophilin complexes from Wüthrich's laboratory (Spitzfaden et al., 1992) highlighted changes of 0.1 ppm for ^1H and 0.5 ppm for ^{15}N. By the former criteria more than 25% of the SH2 residues would be affected by ptyr binding. The latter would not, for example, score interactions of ptyr with either Arg αA2 or βB5 as significant. Since these interactions are well-known and have been independently confirmed by X-ray and NMR data, such a window is likely too discriminating. To make the regions

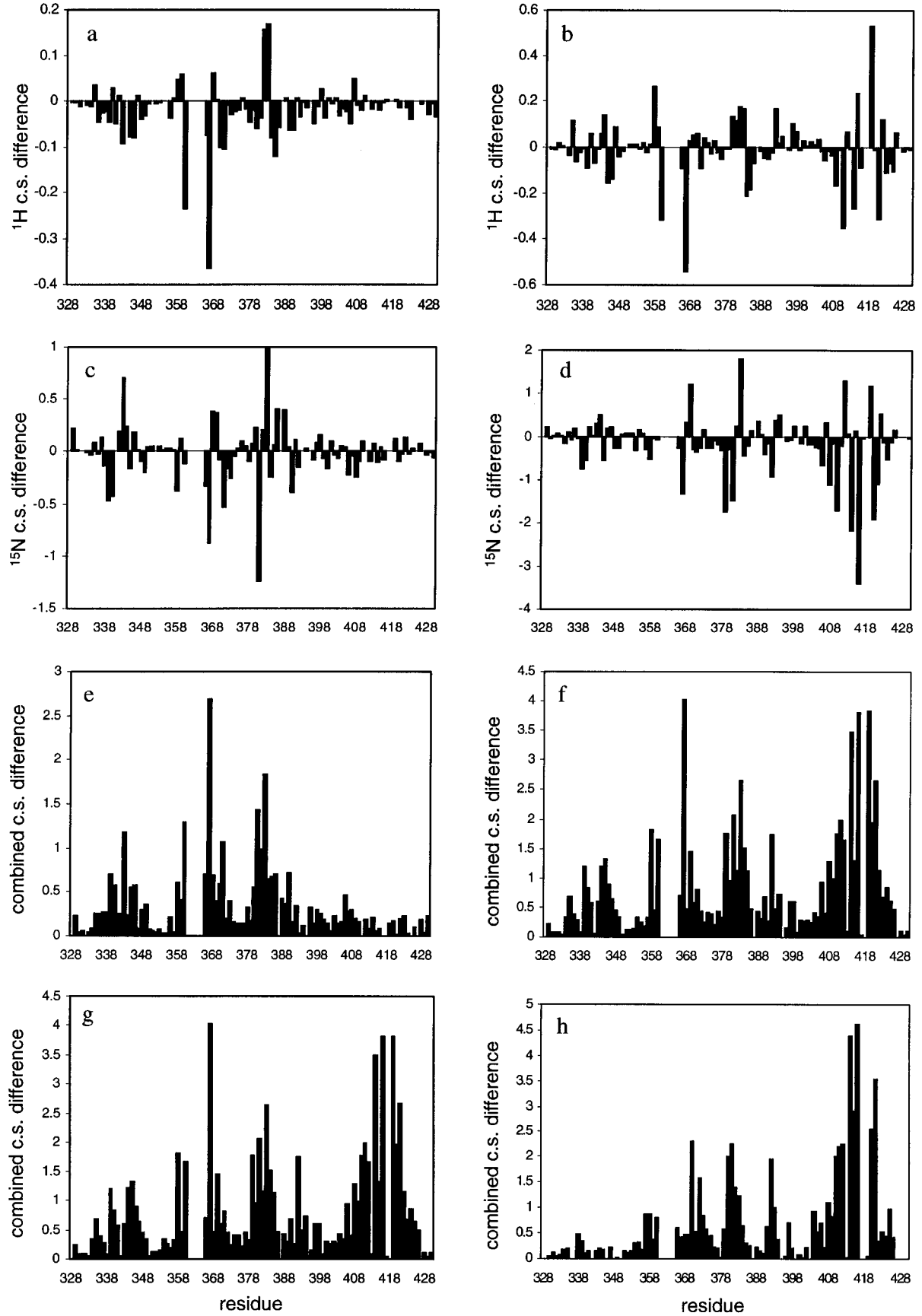

FIGURE 5: Effects of substitution on chemical shifts. Chemical shift differences between uncomplexed SH2 and either Ac-pY-NH_2 (a, c, e) or EEEpYMPGE-NH_2 (b, d, f) are plotted as a function of position in the SH2. Differences in the ^{1}H dimension are shown in (a) and (b); differences in the ^{15}N are shown in (c) and (d). A linear combination of both dimensions ($|\delta(^{15}N) + 5|\delta(^1H)|$) is shown in (e) and (f). Chemical shift differences between EEEpY**G**PME-NH_2 and EEEpYMPME-NH_2 (g) or EEEpYMP**G**E-NH_2 and EEEpYMPME-NH_2 (h). Residues that are not observed are left blank.

in the sequence where chemical shifts have changed easier to see, a linear combination of the absolute values of the ^{1}H and ^{15}N chemical shift changes ($5|\delta(^1H)| + |\delta(^{15}N)|$) is shown by residue in Figure 5e. The different weights for

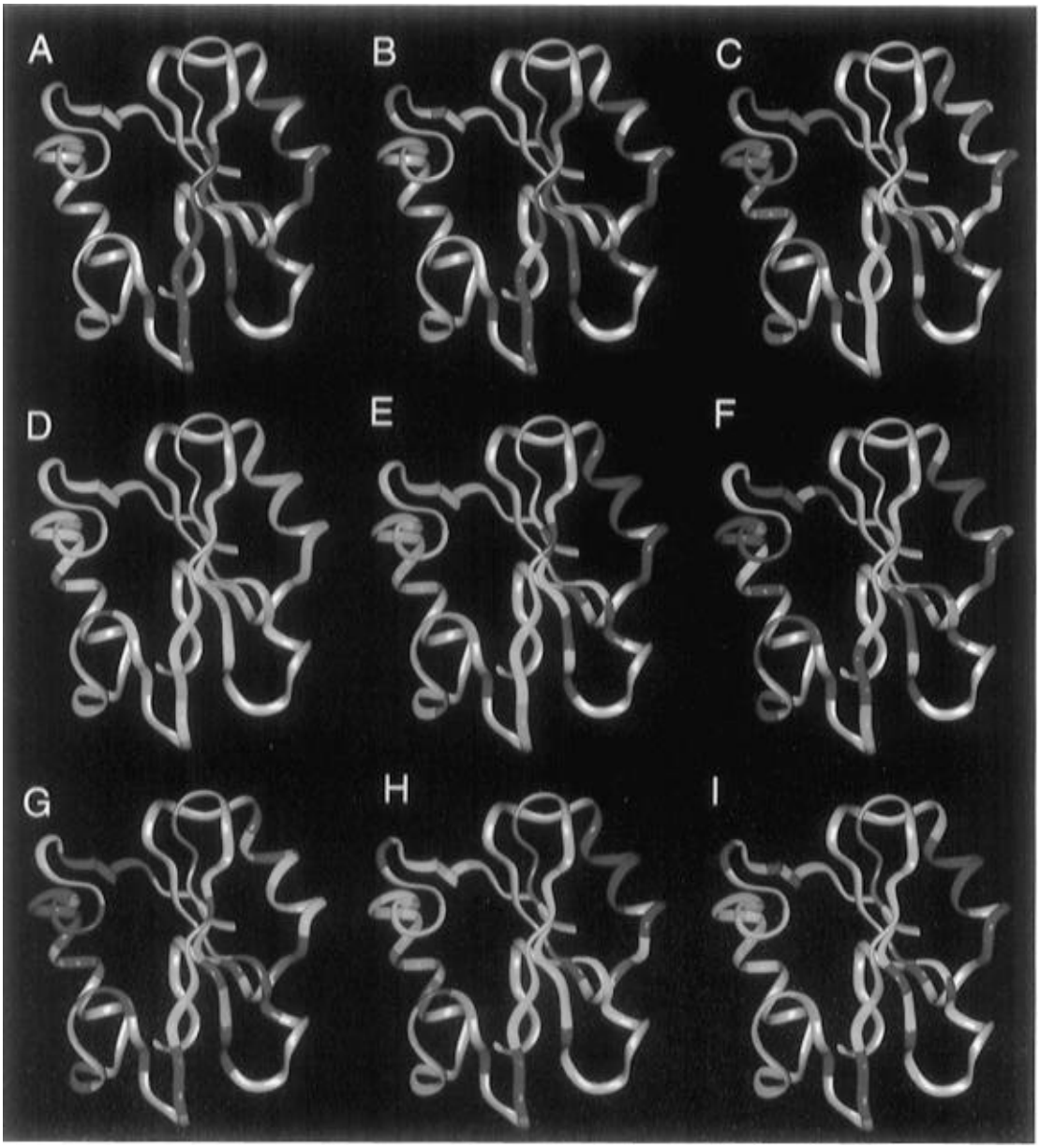

FIGURE 6: Comparison of chemical shift changes. Ribbon diagrams of p85 N-SH2 complexed with (A) Ac-pY-NH_2, (B) pYM-NH_2, (C) EEEpYMPME-NH_2, (D) EEEYMPME-NH_2, (E) EEEpY**G**PME-NH_2, (F) EEEpY**A**PME-NH_2, (G) SVDpYVPML-NH_2 (PDGFr), (H) EEEpYMP**G**E-NH_2, and (I) EEEpYMP**A**E-NH_2. The ribbon diagrams depict p85 N-SH2 oriented as in Figure 1 with αA at the right and αB at the left. (A) shows chemical shift changes for the Ac-pY-N SH2 complex. Residues in (A) are colored blue if they experienced a chemical shift change compared to the free SH2 where $5|\delta(^1H)| + |\delta(^{15}N)|$ was at least 0.45 ppm. In (B) and (C) blue represents chemical shift changes identical to those in the Ac-pY-NH_2 complex, red depicts new chemical shift perturbations not observed in Ac-pY-NH_2, and cyan depicts altered chemical shift changes compared to the Ac-pY-NH_2 complex with $\delta(^1H) > 0.05$ and $\delta(^{15}N) > 0.25$. Green is used for residues whose chemical shift is reverted to the position in free SH2. Color coding for (D−I) is analogous to that for (B) and (C) using the wild-type MT peptide−SH2 complex (C) as a standard.

^1H and ^{15}N reflect the different scales of their chemical shift changes. We have considered chemical shift changes as significant where $5|\delta(^1H)| + |\delta(^{15}N)|$ was greater than 0.45 ppm. In this case, 20 out of 100 observable residues show chemical shift changes when ptyr binds. For chemical shift changes between different complexes, we used a window slightly more stringent than that of Wright: 0.05 and 0.25 ppm for ^1H and ^{15}N, respectively.

The ribbon diagram of Figure 6A shows how binding of Ac-pY-NH_2 induced chemical shift changes in four regions of the SH2: αA, βB, βC, and βD/βD′. Changes in αA (residues S339, R340, V343, E345 and K346) and in βB (residues R358 and A360) were expected from X-ray and NMR structures of several SH2 domains, showing that RαA2 and RβB5 coordinate the ptyr phosphate with their positively charged side chains [e.g., Waksman et al. (1993) and Nolte et al. (1996)]. S339 is affected together with its neighbor R340. An additional series of chemical shift changes were observed in βC residues 366−368 and 371 as well as in βD residues 380−386. Although the BC loop residues are not visible, spectra for all complexes with the exception of the unphosphorylated EEEYMPME-NH_2 show an upfield proton chemical shift of approximately 0.3 and 0.5 ppm for A360 and D367, the residues that flank the BC loop. A possible explanation for these changes would be an aromatic ring current effect from the ptyr ring.

The observed changes defined a region affected by ptyr binding that extends from αA and βB to sequences in βC and βD in the central β-sheet. No changes are observed in the more C-terminal portion of the SH2 where peptide

residues C-terminal to ptyr are thought to bind. Ptyr and phenyl phosphate induced essentially the same HSQC changes as Ac-pY-NH_2 (not shown). The identity of spectral changes with phenyl phosphate and Ac-pY-NH_2 suggests that the chemical shift changes in the central β-sheet caused by Ac-pY-NH_2 binding arise from the ring and the phosphate, not from peptide backbone interactions (not shown).

More distant analogs of ptyr were assessed in the same way. Neither arsanilic acid nor boronic acid derivatives induced chemical shift changes in the HSQC spectra at concentrations up to 5 mM (not shown). The nature of the phosphotyrosine binding region is one of high specificity where steric and electronic changes are not easily tolerated.

N-SH2 Interactions with pYM. pYM was chosen both to probe for possible H-bonds from the pY + 1 and to begin to examine contacts outside the ptyr pocket. The ribbon diagram summary of Figure 6B shows residues with changes similar to those in the the Ac-pY complex (blue) as well as some additional residues now showing chemical shift changes (red). The chemical shift of the residue shown in green (S380) reverted to a position similar to that of the uncomplexed SH2, while the residue in cyan (I383) was shifted differently from the Ac-pY-NH_2 complex.

An H-bond from the +1 amide nitrogen to the βD4 carbonyl has been reported in X-ray structures of different SH2s (p85N, src. lck, syp). *Ab initio* calculations predict ^{15}N chemical shift changes of 0.5−2 ppm for a nitrogen bound to a peptide carbonyl which receives a hydrogen bond (de Dios et al., 1993). The ^{15}N signal of residue βD5 (I381) following βD4 was shifted compared to the uncomplexed SH2 for all ptyr-containing ligands. However, the difference between the pY (−1.24 ppm) and the pYM (−1.48) complex is small so the existence of the H-bond could not be confirmed.

pYM and high-affinity peptide binding induced a strong change for the ^{15}N chemical shift of βD3 (K379). The ^{15}N signal of the neighboring residue S380 (βD4) moves upfield upon pYM and MT peptide binding but downfield on binding N-Ac-pY-NH_2. The ^{15}N signals of residues K419 and V422 in BG experience a downfield shift. This likely represents contribution from the methionine side chain.

Interactions with Peptides Derived from the PI 3′-Kinase Binding Site on Middle T. Figure 4 (bottom) shows a superposition of a section out of the HSQC spectra during the titration of EEEpYMPME-NH_2. Figure 5b,d,f maps changes along the SH2 sequence, and Figure 6C summarizes them on the ribbon diagram by comparison to the Ac-pY-NH_2 complex. The MT peptide induced changes in a substantial number of additional resonances (marked in red) not affected by pY. Binding the MT peptide affects all of the signals influenced by binding of pY and most of those changed by pYM although in some cases chemical shift changes were different (shown in cyan; e.g., S339, E342, E345, and K346 in αA as well as in the FLVR R358 βB5). Changes in the central β-sheet were usually larger than for the pY complex**.** Noticeable modifications were detected for D367, T369, L370, K379, S380, I381, I383, and R386. D367 (βC1) lies deep in the ptyr pocket and flanks the C-terminal side of the BC loop. The nitrogen of T369, two residues downstream, was shifted in the MT complex but not in the pY or pYM complexes. S380 (βD4) and I383 (βD7) are both involved in interactions on either side of the central β-strand. The ^{15}N chemical shift of S380 goes from a modest downfield shift in the ptyr complex to a modest upfield shift in both the MT and the pYM complex. In βD the ^{15}N chemical shift change observed for βD3 (K379) was particularly dramatic. Sizable differences between both pY and pYM and between pYM and MT peptide complexes suggested that it was affected by both the pY +1 side chain and interactions with the +3 residue, which is in agreement with previous X-ray data. A similar conclusion could be reached for I383 on the basis of ^{15}N chemical shift differences among SH2 complexes with pY, pYM, and the MT peptide. X-ray data (Nolte et al., 1996) showed a water bridge from the +3 amide to the peptide carbonyl of K382, which may be reflected here by the effect on the NH of I383.

A new set of alterations not observed in ptyr or pYM complexes extended away from the central β-sheet toward αB. These involved changes in βE, the EF loop, and βF and almost in all residues from the middle of αB through BG. Such effects could have been anticipated from the C-terminal extension of the peptide based on available SH2 structures and genetic analysis. The lack of almost all of these effects in the pYM complex proves their connection to interactions originated by the extension of the peptide. The largest ^{15}N chemical shift change for MT peptide binding (−3.4 ppm) was observed for Y416. The recent X-ray structure (Nolte et al., 1996) shows that the side chain of this residue rotates out of the pY +3 pocket upon peptide binding. In this case alterations of ϕ, ψ, and χ_1 are probably the main cause of ^{15}N chemical shift changes, because the ^{1}H chemical shift which is sensitive to polar interactions remains unaffected. Large ^{15}N shifts are also observed across αB and BG for residues Y408, N410, S412, A414, L420, D421, and K423−L425. Interestingly, residues K419 (BG8) and V422, affected when pYM bound, show much greater ^{15}N downfield shifts upon binding of the MT peptide. Such residues appear to be responsive to both +1 and +3 interactions. Previous data suggested the importance of the EF loop in coordination of +3 (Yoakim et al., 1994). Not only are S393 (EF1) and D394 shifted by peptide binding, but the upfield shift on F392 suggests participation of this residue in the coordination of +3. In fact, X-ray data shows that the carbonyl of this residue is involved in a water bridge between the pY +3 NH and the peptide carbonyls of K382 and D394 (Nolte et al., 1996).

Unphosphorylated MT Peptide. Unphosphorylated EE-E**Y**MPME-NH_2 was titrated to saturation for comparison to EEE**pY**MPME-NH_2. The chemical shift changes are listed in Table 2 of Supporting Information. Both biological and biochemical analyses indicate that this peptide binds poorly to the SH2. Figure 6D displays the chemical shift changes observed for EEE**Y**MPME-NH_2 compared to EEE**pY**MPME-NH_2. For many residues (green) chemical shifts reverted to those of the free SH2. However, the interaction caused chemical shift changes both in the central sheet and in the EF loop, αB and BG of the +3 pocket. Where chemical shift changes were different (cyan), they were usually smaller than when the phosphorylated form of the peptide bound. Chemical shift changes around αA2 where the phosphate binds virtually disappeared; the chemical shift change for the FLVR arginine (βB5) was in the opposite direction (from −0.51 ppm for EEEpYMPME to 0.27 ppm for EE-EYMPME). The chemical shift changes of residues surrounding the BC loop were different from those in the phosphorylated peptide. The remarkable ^{1}H upfield shift for A360 and D367, the edges of the BC loop, disappeared. The ^{15}N downfield shift for the signal of Y368 (βC2) is

transformed into an upfield shift. Many chemical shift changes in βD were smaller. However, βD4 (S380) and βD6 (K382) which flank the aromatic ring showed larger ^{15}N chemical shift changes. In the case of the +3 pocket, the large chemical shift change for Y416, for example, was substantially reduced. The sum of these observations suggests that the missing interaction with the ptyr phosphate leads to a modified set of interactions, insufficient to achieve high-affinity binding.

Other High-Affinity MT Peptides. Examination of other peptides (EEEpYMPME**DLYLDIL**-NH_2 and EEEpYM**G**ME-NH_2) that compete well in the binding assay showed HSQC spectra very similar to that observed for the MT peptide EEEpYMPME (Table 2, Supporting Information). With very few exceptions the longer version of the middle T peptide extending to middle T residue 326 showed the same influences on chemical shifts as the shorter one. One notable exception was that of the EF loop residue S393. In the longer peptide this residue showed a dramatic chemical shift change (^{1}H 0.55 ppm/^{15}N 2.34 ppm) but only a very modest one in EEEpYMPME-NH_2 (^{1}H 0.018 ppm/^{15}N 0.395 ppm). This and changes in the neighboring residue D394 suggest that the extension of the peptide stretches across the EF loop region. Another noticeable difference was observed for Y416 of BG for which the ^{15}N shift was even larger, although the other residues in the BG loop remain largely unaffected. Additional changes were observed in βB (V357, A360) and small changes in both βC and βD. Substituting G for M at +2 had little effect on the HSQC spectrum. This supports the lack of importance of the +2 residue for high-affinity binding.

PDGFr Peptide. The PDGFr sequence around 751 (SVDpY**V**PML-NH_2) binds to the SH2 with high affinity. In competition assays with middle T, this peptide gave an IC_{50} of 8 μM. Figure 6G summarizes the chemical shift differences compared to the wild-type middle T peptide. Residues affected by extension of the MT peptide to include the +3 methionine were essentially the same here (blue), consistent with the +3 methionine in the PDGFr sequence. In general, differences were smaller compared to those observed for the low-affinity peptides with substitutions in the +1 and +3 positions reported later in this work. From the end of AA through the first seven residues of αA there were minor differences. In the central β-sheet βD3 (K379) was significantly different from the wild-type middle T peptide as were two residues in BG (K419, L420). These results are not surprising, because the signals of K379 and K419 changed substantially between pY and pYM complexes and were therefore attributed to +1 interactions. It seems reasonable that the valine in pY +1 of PDGFr affects these residues differently than the methionine of middle T.

Effects of Substitution at +1 or +3 Positions. The initial goal was to assess side chain contributions by comparison to glycine-substituted peptide−SH2 complexes. Figure 5g,h depicts the differences in chemical shift changes when glycine is substituted for methionine at +1 or +3, respectively.

As noted above (Table 1), substitution of G for M in pY +3 (EEEpYMP**G**E-NH_2) caused a dramatic decrease in affinity. As can be seen in Figure 6H, there were substantial differences from the wild-type peptide complex. Many residues (shown in green) that correlate with the coordination of the +3 methionine side chain revert to positions similar to those of the uncomplexed form. These include the NMR signals of residues F392, D394, T397, and F398 of the EF loop region and N406, Y408, N410, and E411 in αB. Other residues (cyan) in αB and the BG loop showed modified effects compared to those caused by MT wild type (R409 in αB; Q415, Y416, L420−V422, L424, and L425). The large chemical shift change observed for Y416 was changed from a large ^{15}N upfield to a modest downfield shift.

Significantly, a series of new or different chemical shift changes compared to MT peptide binding were also observed in regions associated with pY or +1 coordination. These include changes in βC, such as T368 (βC2)−K374, in βD K379 (βD3)−F384, and in βD′ K386. K382 and I383 in βD were both affected by ptyr binding. The chemical shifts of these peaks in EEEpYMPGE-NH_2 differ from both those in the uncomplexed SH2 and those in the complex with EEEpYMPME-NH_2. Even the chemical shifts of the FLVR arginine (βB5) and the preceding valine were different from that in the MT peptide complex. This strongly suggests interdependence of the pY +3 and the pY binding region.

Intriguing chemical shift changes were observed when the +1 methionine was changed to glycine in the MT peptide (EEEpY**G**PME-NH_2) (Figure 6E). There were many differences from the wild-type peptide complex. This is in good agreement with the loss of high-affinity binding for the +1 glycine-substituted peptide. Given that the PDGF receptor peptide with valine at +1 showed changes in the central sheet, it was not surprising that EEEpY**G**PME-NH_2 also showed changes there. The very striking result was that residues associated with binding at the +3 position showed substantial chemical shift changes even though the peptide retained the +3 methionine. The chemical shifts (shown in green) of a substantial number of signals in the EF loop region (F392−D394, T397, F398), in αB (N406 and Y408−S412), and in BG (Q415, L420−D421, and K423−Y426) were all reverted to their position in the uncomplexed SH2. Other chemical shift changes (cyan) in BG were reduced (A414, Y416, K419) or reverted (V422). The chemical shift change for Y416, previously attributed to a large rearrangement required to shape the pY +3 pocket, was also significantly reduced. Changes in K419 and V422 might have been expected because these residues showed altered shifts when pYM was used for comparison to pY. Changes in the central β-sheet were also observed. None of the effects observed for MT peptide binding in βD remained unchanged. Significant differences were observed for the ^{15}N chemical shifts of K379 (βD3) and I383 (βD6). The effect on K382 (βD5) suggested a change in the nature of the interaction of this residue; the change on the ^{15}N chemical shift is eliminated and the proton chemical shift is increased. Altered chemical shift changes compared to the MT peptide complex were also found throughout βC (D367, T369, L370, and L372). Considered together, these changes upon altering +1 included residues that show strong changes when ptyr (e.g., βD6 K382) binds and residues that appear to be strongly influenced by the extension of the peptide to include the +3 position such as I383 (βD7) or D367 (βC1).

In contrast to chemical shifts of residues such as K382, affected by both ptyr and the +1 side chain, chemical shifts from positions where the tyrosine phosphate interacts were essentially unchanged. The effects on R340 (αA2) and on the βB5 FLVR arginine were rather similar to those of the wild-type peptide, as were the chemical shifts throughout αA and βB.

To obtain some sense of how much of the hydrophobic side chain is needed in the +1 and +3 positions, peptides containing alanine were employed. For the peptide with the +1 position substituted with alanine (Figure 6F), many of the differences seen between the +1 glycine-substituted peptide and the MT peptide disappeared. Comparing Figure 6E to Figure 6F, the overall impression is that alanine at the +1 position was sufficient to permit many of the chemical shift changes seen with the wild-type peptide (blue) but that glycine at +1 was not. For example, chemical shift changes from the second half of αB through Y416 in BG looked like those of the wild-type peptide. Not surprisingly, chemical shift changes for K419 were different to those of the wild-type peptide. K419 had previously been associated with interactions with the +1 side chain. Where most effects in the EF region were reverted for the +1 glycine-substituted peptide, they were maintained for the alanine-substituted version. Changes in the central β-sheet also looked more similar than those for the wild-type peptide although chemical shift changes were smaller. These results are in good agreement with the relatively high affinity of EEEpYMPME-NH_2 in the MT competition assay.

Results for alanine substitution at +3 were different than for +1 alanine substitution. Figure 6I shows that the +3 Ala peptide complex had many differences from the wild-type peptide. Comparison of Figure 6H to Figure 6I shows considerable similarity between peptides with alanine or glycine at +1. Large chemical shift changes compared to the uncomplexed SH2 were observed in the central β-sheet (L370−K374 in βC and K379−I383 in βD) where the MT complex had either smaller or no changes. These included residues affected by both +1 and ptyr binding. For residues in αB and the first part of BG chemical shift changes were much smaller than for the wild-type peptide complex or reverted to the position in uncomplexed SH2. Signals of residues in the EF loop were also reverted to the position in uncomplexed SH2, with the exception of S393, for which the ^{15}N chemical shift was very different from that in both uncomplexed SH2 and the wild-type peptide−SH2 complex.

DISCUSSION

The goal of this work was to monitor the interactions of an SH2 domain with a large collection of ptyr ligands to dissect some of the subtleties of SH2 behavior. NMR analysis of chemical shifts in HSQC spectra was selected as the method of choice. Chemical shift changes have often been used to map protein−peptide interactions (Spitzfaden et al., 1992; Chen et al., 1993; Combs et al., 1996). A general advantage of chemical shift analysis is that one can observe not only residues directly interacting but also those that are perturbed secondary to the primary interaction. A peptide titration of the SH2 using HSQC can be obtained rapidly. With assignments available, the analysis of chemical shift changes is quite fast. Therefore, it is feasible to compare a whole series of ligands with respect to their binding properties.

Although quantitative dependence of amide ^{15}N or ^{1}H chemical shifts on molecular structure and protein−ligand interactions is complex, chemical shifts provide an advantage of considerable sensitivity. Observations of a correlation between secondary structure and H^{α}, H^{β}, and C^{α} chemical shifts led to increased interest in chemical shifts in proteins (Oldfield, 1995; Wishart et al., 1994, 1995). Recent advances in quantum chemical calculations provide a better theoretical understanding of chemical shifts, including ^{15}N chemical shifts of backbone amides. De Dios has shown that most ^{15}N chemical shifts in proteins can be predicted by quantum chemical calculations employing H-bonds from the HN atoms, H-bonds to the carbonyl of the preceding peptide, and ϕ and χ_1 torsional angles as variable parameters (de Dios et al., 1993). The largest ^{15}N chemical shift effects were reported to arise from hydrogen bonds involving the HN (1−13 ppm) whereas shifts induced by hydrogen bonding to the preceding peptide carbonyl do not exceed 2 ppm. Large effects (±10 ppm) were also reported for variations of ϕ and χ_1 torsion angles. In fact, in the absence of strong direct H-bonds to the observed nitrogen, the largest contribution comes from the geometrical arrangement of the amino acid. Several authors have determined chemical shift surfaces depicting ^{15}N chemical shift as a function of ϕ and χ_1 (Gluska et al., 1989; Wishart et al., 1991), which yield better results if determined for individual amino acids (Le & Oldfield, 1994).

A disadvantage of the approach is ambiguity about the origin of the change that has occurred. Changes in torsion angles, for example, are clearly structural. Changes of hydrogen bond strengths involving the NHs within the protein can also be regarded as structural changes. Chemical shift positions and line shapes also could depend on affinities or saturation, which would not represent structural changes. The titrations of Figure 4 provide a simple example of this possibility. However, this seems unlikely because all of our analysis is carried at peptide concentrations where no more chemical shift changes occur upon further peptide addition. Another possibility is that electrostatic effects contribute to the chemical changes observed. If this were the case, then chemical shift alterations could simply reflect changes of the electrostatic environment independent of a structural change. It is difficult to know how important such effects might be. Clearly, the introduction of the phosphate, for example, does not seem to have global effects on chemical shifts across the SH2.

X-ray diffraction of the p85 N-SH2 appeared as this work was nearing completion. It allows valuable comparison. There is substantial agreement between the two approaches, providing reassurance about the value of the chemical shift analysis. The αA2 and βB5 arginines involved in ptyr phosphate interactions and residues βD4 and βD6 involved in supporting the ring showed effects using both methods. Similarly, the associations of the +1 position with βD3 (K379), βD5 (I381), and BG8 (K419) seen in the X-ray analysis could all be observed from changes in spectra among pY, pYM, and the longer peptides. The added interaction between the +1 valine of PDGFr and BG9 (L420) could also be confirmed by large chemical shift differences between the PDGFr and the MT peptide complexes. The very large rearrangement in BG5 (Y416) reported by Nolte and colleagues was reflected in the largest ^{15}N chemical shift change caused by binding MT peptide. In the X-ray structure Y416 changes position from between L420 and F392 to between F398 and Y408. The NMR data show that F392 and F398 as well as Y408 and L420 experience chemical shift changes.

However, NMR chemical shift analysis gives results somewhat different from those of X-ray diffraction in a number of areas. We observed only a very small ^{15}N chemical shift effect for the H-bond from the M + 1/V + 1 backbone amides and the peptide carbonyl of βD4 (L/S380).

Examination of the carbonyl chemical shift in a ^{13}C-labeled sample might be useful here. L413 (BG2) was reported to be one of the residues involved in the +3 interaction, but no sign of this interaction could be observed by looking at chemical shift changes. It is possible that such alterations occur without change of the magnetic environment of the amide. The short N-terminal amphipathic helix reported before the conserved tryptophans was also not observed even though our construct contained even a few more residues than that of Nolte and colleagues. This additional helix may be induced by the crystallization conditions or by a difference in sequence.

There is also a substantial collection of residues showing NMR changes that were not discussed after the X-ray analysis. Many additional changes were seen in the region where +3 is found, the EF, βB, and BG loop areas. Some of these certainly represent concerted rearrangements of side chains induced by the displacement of the BG loop. However, it seems unlikely that all of the changes result from movement of BG. Additional changes were seen in the more central part of the molecule, in αA, in βC (D367), and in βD (I383 and residues C-terminal to it). Similarly, alterations in EF and BG for the longer MT construct EEEpY$_{315}$-MPMEDLYLDIL-NH_2 compared to the shorter EEEpY$_{315}$-MPME-NH_2 were also in agreement with X-ray structures which mentioned S393 and Y416 as pY +4 contacts. However, by NMR we observe additional changes in βB (V357, A360) and small changes in both βC and βD.

What picture emerges from the NMR results? The prong and socket model of SH2 function originally proposed from X-ray structures (Waksmann et al., 1993) describes major sites of protein−peptide interaction: the phosphotyrosine binding site and a hydrophobic site which coordinates the residues C-terminal to the ptyr, particularly the +3 residue but also the +1. The NMR data support the idea that high-affinity binding requires synergistic interplay of all contributing interactions.

Ptyr binding showed chemical shift changes on residues usually associated with phosphotyrosine binding. Both "active site" arginines (αA2 R340 and βB5 R358) were affected and so were residues that are known (Nolte et al., 1996) to flank the benzene ring, βD4 (S380) and βD6 (K382). βD5 (I381) was reported to provide some support for the tyrosine ring in src and lck SH2 domains, although X-ray structures of p85 N-SH2 rule out direct amino−aromatic interaction for p85 N-SH2.

Comparison of HSQC spectra of pY and pYM showed that chemical shifts of most residues in βC and βD were different. This suggests that the interactions on the central β-sheet are apparently altered by the +1 methionine. It should be emphasized that no participation of residues in EF, βB, or the beginning of BG was observed for either pY or pYM.

The transition from pYM to a MT peptide (EEEpYMPME-NH_2) again caused moderate changes on the central β-sheet. For example, the chemical shift of the FLVR arginine βB5 is different. The behavior of K379 in βD is particularly interesting. It was not affected in the pY complex. Compared to uncomplexed SH2, K379 showed a modest ^{15}N chemical shift change in the pYM complex (−0.49 ppm) and a large effect in the MT peptide complex (−1.75 ppm). MT peptide binding also caused a large number of changes around the EF loop and in the BG loop which can be attributed to pY +3 interactions. Some of the chemical shift changes observed in the EF loop provide rationales for the properties of existing mutants. For example, EF loop residues S393 (EF1), D394, and P395 are all known to affect the binding properties of the SH2 and to be involved in selection at +3 (Yoakim et al., 1994). NMR data emphasize the importance of EF loop interactions by the participation of two adjacent residues, S393 and D394; proline 395 is not observed in proton-detected $^1H-^{15}N$ HSQC spectra. Further changes in EF and BG when a longer MT construct, EEEpY$_{315}$MPMEDLYLDIL-NH_2, was used were in agreement with both X-ray results which mentioned S393 and Y416 as pY +4 contacts and the observation of a small increase of affinity.

Effects by extension of the ligand to include +3 even caused changes in the ptyr binding region beyond those seen in the central sheet. Residues of αA including those affected by the phosphotyrosine were affected quite differently when the wild-type middle T peptide was used (Figure 6A vs 6C). Differences in the N-terminal end of αA (S339, R340, and E341) with the MT and PDGFr peptides as well as differences between wild-type and substituted middle T peptides around βB5 (R358) also suggest changes in the arrangement of the ptyr and its coordinating residues. A change on the edge of the BC loop residues (A360 βB6) attributed to the ptyr interaction was affected by residues C-terminal to the ptyr in a manner varying even with the +3 side chain. X-ray diffraction data also point to changes in orientation of the ptyr for the c-kit and PDGFr peptide complexes.

The interactions involving the +1 and +3 sites are even more interesting. Substitution of either methionine +1 or methionine +3 with glycine raised the concentration of peptide required in competition experiments above millimolar (Table 1). Peptide fishing experiments have given rise to the notion that the binding effects of the +1 position, the +3 position, and the phosphotyrosine are more or less discrete (Songyang et al., 1993, 1994). Comparisons of pY, pYM, and the peptides clearly confirm that the residues involved in interactions with the pY +3 position are generally found in the EF loop, αB, and BG. What is surprising is that the chemical shifts of these residues depend strongly on the rest of the peptide. Although one might have imagined that the role of the ptyr would have been restricted to residues of αA and the central sheet, the unphosphorylated wild-type middle T peptide showed a very different pattern of chemical shifts through the EF loop, αB, and BG. Removal of the tyrosine gave a peptide (MPME) that showed no interaction in the NMR. It is worth pointing out that adding MPME plus phenyl phosphate did not cause shifts in the +3 region, suggesting that physical connection between pY and MPME is required between the sites.

Changes in the peptide sequence at either +1 or +3 had dramatic effects in regions associated with +3. That substitutions at +3 (Figure 6H,I) caused alterations in these residues was certainly expected. Glycine and alanine +3 substituted peptides gave very similar results. S393 in the EF loop appears involved in backbone interactions because it showed a substantial ^{15}N shift in both glycine- or alanine-substituted peptides. Very unexpected were the large effects on the +3 region caused by substituting glycine for methionine at +1 (Figure 6E). Most of the chemical shifts in the region looked like those for uncomplexed SH2. Moreover, the +1 substituted peptides gave very different results

for A versus G substitution. The alanine-substituted peptide looked very much like the wild type in EF, αB, and BG through 416. This suggests that the first methylene in the +1 position is critical for forming the appropriate +3 pocket. It was therefore not surprising that the PDGFr peptide which has a valine in +1 looked quite similar in this region to the wild-type middle T peptide.

The +1 position of the peptide makes a substantial contribution to peptide interaction with the SH2 as seen from the binding data of Table 1. Comparisons between pY and pYM call attention to K419 and V422 of BG, residues toward the C-terminus of βC, and residues K379 and I383 of βD. In the case of K419 and V422, chemical shifts depend on the rest of the peptide. The effect of pYM is different from that of EEEpYMPME-NH_2. The chemical shift changes even depend on the tyrosine phosphate; EEEYMPME-NH_2 gives different results from EEEpYMPME-NH_2. A similar picture is seen in the central β-sheet. K379 βD3 showed substantial change on going from pY to pYM. Removing the phosphate from the wild-type middle T peptide changed the ^{15}N chemical shift by 1.06 ppm compared to the chemical shifts of MT peptide, even though pY by itself had no effect. These chemical shifts are significantly responsive to changes at +1. Substitutions at +3 caused a change compared to the MT peptide complex for V422, K379, and I383, all of which are associated with +1 interaction. The sensitivity of the chemical shifts affected by +1 to what is happening in the peptide at other positions provides an explanation for a genetic puzzle. EF loop mutants such as P395S and S393 reduced the ability to bind middle T but not the PDGF receptor. When the mutant was examined for its ability to bind peptides from a library, it was found to have lost discrimination at +3 but intriguingly to show altered discrimination at +1.

Specificity as measured by peptide selection suggests that M,V, I, or E is preferred at the +1 position and there is a strong selection for methionine at +3. Nolte and colleagues have attributed specificity at +3 solely to steric effects. While steric exclusion may contribute to specificity, it does not explain why a smaller residue should not fit. Alteration of the peptide from M to A in +3 shows that the origin of +3 specificity is more complex. Ala is smaller than Met and certainly has to fit into the +3 pocket. Yet the affinity was much lower. The NMR data showed alterations for many residues in EF, αB, BG, and even the central β-sheet associated with +3. One possibility is that incomplete rearrangement of residues such as Y416 leaves the protein in an energetically less favorable conformation, which reduces the affinity for the peptide. The situation at +1 is somewhat different. Substitution of alanine and glycine gave quite different results. The methyl of alanine in +1 is sufficient to achieve substantial, if somewhat reduced, affinity. NMR analysis showed strikingly that the +1 alanine-containing peptide restored the chemical changes associated with +3 that were lost in the +1 glycine-containing peptide. For example, Y416 showed exactly the same chemical shift in the alanine-containing peptide as for wild type. The residues affected by the alanine substitution are in the end of the BG loop, where the side chain cannot reach. This might account for the somewhat reduced affinity.

The studies presented here show the value of chemical shift analysis for evaluating ligand interactions. Better theoretical understanding of the origin of ^{1}H and ^{15}N chemical shifts will aid this type of analysis and permit more quantitative conclusions in the future.

ACKNOWLEDGMENT

We thank Jim Baleja for a critical reading of the manuscript.

SUPPORTING INFORMATION AVAILABLE

Tables showing (1) ^{1}H and ^{15}N chemical shifts of p85 N-SH2 at pH 6.9 and 308.3 K and (2) ^{1}H and ^{15}N chemical shift changes for p85 N-SH2 at pH 6.9 and 308.3 K upon binding of different compounds (7 pages). Ordering information is given on any current masthead page.

REFERENCES

Bax, A., Ikura, M. Lay, L., Torchia, D., & Tschudin, R. (1990) *J. Magn. Reson. 86*, 304−318.
Booker, G. W., Breeze, A. L., Downing, A. K., Panayotou, G., Gout, I., Waterfield, M. D., & Campbell, I. D. (1992) *Nature 358*, 684−687.
Campbell, I. D., Dobson, C. M., Jeminet, G., & Williams, R. J. P. (1974) *FEBS Lett. 49*, 115−119.
Cantley, L. C., Auger, K. R., Carpenter, C., Duckworth, B., Graziani, A., Kapeller, R., & Soltoff, S. (1991) *Cell 64*, 281−302.
Carmichael, G., Schaffhausen, B. S., Mandel, G., Liang, T. J., & Benjamin, T. L. (1984) *Proc. Natl. Acad. Sci. U.S.A. 81*, 679−683.
Carpenter, C., Duckworth, B., Auger, K., Cohen, B., Schaffhausen, B. S., & Cantley, L. C. (1990) *J. Biol. Chem. 265*, 19704−19711.
Chen, Y., Reizer, J., Saier, M. H. J., Fairbrother, W. J., & Wright, P. E. (1993) *Biochemistry 32*, 32−37.
Cohen, B., Liu, Y., Druker, B., Roberts, T. M., & Schaffhausen, B. S. (1990a) *Mol. Cell. Biol. 10*, 2909−2915.
Cohen, B., Yoakim, M., Piwnica-Worms, H., Roberts, T. M., & Schaffhausen, B. S. (1990b) *Proc. Natl. Acad. Sci. U.S.A. 87*, 4458−4462.
Cohen, G., Ren, R., & Baltimore, D. (1995) *Cell 80*, 237−248.
Comba, A., Kapoor, T., Feng, S., Chen, J., Daude-Snow, L., & Schreiber, S. (1996) *J. Am. Chem. Soc. 118*, 287−288.
De Dios, A. E., Pearson, J. G., & Oldfield, E. (1993) *Science 260*, 1491−1496.
Eck, M. J., Shoelson, S. E., & Harrison, S. C. (1993) *Nature 362*, 87−91.
Escobedo, J. A., Kaplan, D. R., Kavanaugh, W. M., Turck, C. W., & Williams, L. T. (1991) *Mol. Cell. Biol. 11*, 1125−1132.
Fantl, W. J., Escobedo, J. A., Martin, G. A., Turck, C. W., del Rosario, M., McCormick, F., & Williams, L. T. (1992) *Cell 69*, 413−423.
Freund, R., Dawe, C. J., Carroll, J. P., & Benjamin, T. L. (1992) *Am. J. Pathol. 141*, 1409−1425.
Glushka, J., Lee, M., Coffin, S., & Cowburn, D. (1989) *J. Am. Chem. Soc. 111*, 7716−7722.
Hatada, M., Lu, X., Laird, E., et al. (1995) *Nature 377*, 32−38.
Hensmann, M., Booker, G. W., Panayotou, G., Boyd, J., Linacre, J., Waterfield, M., & Campbell, I. (1994) *Protein Sci. 3*, 1020−1030.
Kashishian, A., Kazlauskas, A., & Cooper, J. (1992) *EMBO J. 11*, 1373−1382.
Ladbury, J., Lemmon, M., Zhou, M., Green, J., Botfield, M., & Schlessinger, J. (1995) *Proc. Natl. Acad. Sci. U.S.A. 92*, 3199−3203.
Le, H. & Oldfield, E. (1994) *J. Biomol. NMR 4*, 341−348.
Lee, C., Kominos, D., Jacques, S., Margolis, B., Schlessinger, J., Shoelson, S., & Kuriyan, J. (1994) *Structure 2*, 423−438.
Marengere, L. & Pawson, T. (1994) *J. Cell Sci., Suppl. 18*, 97−104.
Marion, D. & Wüthrich, K. (1983) *Biochem. Biophys. Res. Commun. 113*, 967−974.
Marion, D., Driscoll, P. C., Kay, L. E., Wingfield, P. T., Bax, A., Gronenborn, A. M., & Clore, G. M. (1989) *Biochemistry 28*, 6150−6156.

Messerle, B., Wider, G., Otting, G., Weber, C., & Wüthrich, K. (1989) *J. Magn. Reson. 85*, 608−613.
Nolte, R., Eck, M., Schlessinger, J., Shoelson, S., & Harrison, S. (1996) *Nat. Struct. Biol. 3*, 364−374.
Oldfield, E. (1995) *J. Biomol. NMR 5*, 217−225.
Otting, G. (1993) *Curr. Opin. Struct. Biol. 3*, 760−768.
Overduin, M., Mayer, B., Rios, C. B., Baltimore, D., & Cowburn, D. (1992) *Proc. Natl. Acad. Sci. U.S.A. 89*, 11673−11677.
Pascal, S., Singer, A., Gish, G., Yamazaki, T., Shoelson, S., Pawson, T., Kay, L., & Forman-Kay, J. (1994) *Cell 77*, 461−472.
Pascal, S., Yamazaki, T., Singer, A., Kay, L., & Forman-Kay, J. (1995) *Biochemistry 34*, 11353−11362.
Payne, G., Stolz, L., Pei, D., Band, H., Shoelson, S., & Walsh, C. (1994) *Chem. Biol. 1*, 99−105.
Schaffhausen, B. (1995) *Biochim. Biophys. Acta 1242*, 61−74.
Schlessinger, J. (1994) *Curr. Biol. 4*, 25−30.
Shoelson, S. E., Sivaraja, M., Williams, K. P., Hu, P., Schlessinger, J., & Weiss, M. A. (1993) *EMBO J. 12*, 795−802.
Songyang, Z., Shoelson, S., Chauduri, M., Gish, G., Pawson, T., Haser, W., King, F., Roberts, T., Ratnofsky, S., Lechleider, R., Neel, B., Birge, R., Fajardo, J., Chou, M., Hanafusa, H., Schaffhausen, B., & Cantley, L. (1993) *Cell 72*, 767−778.
Songyang, Z., Shoelson, S. E., McGlade, J., Olivier, P., Pawson, T., Bustelo, X. R., Barbacid, M., Sabe, H., Hanafusa, H., Yi, T., et al. (1994) *Mol. Cell. Biol. 14*, 2777−2785.
Spitzfaden, C., Weber, H. P., Braun, W., Kallen, J., Wider, G., Widmer, H., Walkinshaw, M. D., & Wüthrich, K. (1992) *FEBS Lett. 300*, 291−300.
Valius, M., & Kazlauskas, A. (1993) *Cell 73*, 321−334.
Waksman, G., Shoelson, S. E., Pant, N., Cowburn, D., & Kuriyan, J. (1993) *Cell 72*, 779−790.
Wishart, D. S. & Sykes, B. D. (1994) *Methods Enzymol. 239*, 363−392.
Wishart, D. S., Sykes, B. D. & Richards, F. M. (1991) *J. Mol. Biol. 222*, 311−333.
Wishart, D. S., Bigam, C. G., Holm, A., Hodges, R. S., & Sykes, B. D. (1995) *J. Biomol. NMR 5*, 67−81.
Xu, R., Word, J., Davis, D., Rink, M., Willard, D., & Gampe, R. (1995) *Biochemistry 34*, 2107−2121.
Yoakim, M., Hou, W., Liu, Y., Carpenter, C. L., Kapeller, R., & Schaffhausen, B.S. (1992) *J. Virol. 66*, 5485−5491.
Yoakim, M., Hou, W. M., Liu, Y. L., Songyang, Z., Cantley, L., & Schaffhausen, B. (1994) *Mol. Cell. Biol. 14*, 5929−5938.
Zhou, M.-M., Meadows, R. P., Logan,T. M., Yoon, H. S., Wade, W. S., Kodimangalam, R. S., Burakoff, S. J., & Fesik, S. W. (1995) *Proc. Natl. Acad. Sci. U.S.A.* 92, 7784−7788.

BI961783X